ISSN 1392–1320 MATERIALS SCIENCE (MEDŽIAGOTYRA). Vol. 20, No. 1. 2014

Modeling of Nitrogen Penetration in Medical Grade CoCrMo Alloy during Plasma Nitriding

Arvaidas GALDIKAS [1, 2] *, Akvilė PETRAITIENĖ [1]

[1] *Physics Department, Kaunas University of Technology, Studentų St. 50, LT-51368 Kaunas, Lithuania*
[2] *Department of Physics, Mathematics and Biophysics, Lithuanian University of Health Sciences, Eivenių 4, LT-50166 Kaunas, Lithuania*

crossref http://dx.doi.org/10.5755/j01.ms.20.1.3458

Received 06 February 2013; accepted 08 July 2013

For analysis of plasma nitriding process and nitrogen penetration into CoCrMo alloy the trapping-detrapping model is applied. This model is commonly used for analysis of stainless steel nitriding, however, in this work it is shown that the same nitrogen penetration mechanism takes place in CoCrMo alloys. From the fitting of experimental curves, taken from literature, it is found by the proposed model that diffusion coefficient depends on nitrogen concentration according to Einstein-Smoluchowski relation $D \propto 1/C_N$. The diffusion coefficients for 400°C temperature nitriding of in CoCrMo are calculated. The shape of nitrogen depth profile curves are analyzed showing influence of different parameters such as detrapping activation energy, chromium concentration, etc.
Keywords: CoCr alloy; nitriding; concentration dependant diffusion; trapping-detrapping model; kinetic modeling.

1. INTRODUCTION

CoCr alloys are widely used in medicine because, these alloys are characterized by a good elasticity and high resistance of corrosion, what is very important for the biomaterials. Cobalt-chromium alloys are stronger and have better corrosion resistance than stainless steel. The molybdenum is added to produce finer grains which results in higher strengths after casting or forging [1, 2]. For joint implant, these alloys are usually composed of 30 % – 60 % cobalt, 20 % – 30 % chromium, 7 % – 10 % molybdenum [3]. It has face-centered cubic (fcc-γ) accompanying by some amount of hexagonal-closed packed (hcp-ε) structure. The ε phase exists as thin plates (bands) in the fcc-γ CoCrMo matrix [4].

It is very important to improve wear resistance and in the same time to keep high corrosion resistance of biomaterials. For the last two decades cobalt chrome and titanium alloy prosthetic knee and hip replacements have been treated by ion implantation to increase the wear resistance and hence reduce the possibility of osteolysis. The life spans of such prostheses are still limited (on average about 8 – 10 years) due to the inherent physical limitations of the technique [5]. An increase in the surface hardness and a reduction of the wear rate is still desirable to improve the biocompatibility [6]. Nitriding improves wear, corrosion resistance and fatigue strength [1]. A good corrosion resistance is determined by chromium concentration. Chromium is responsible for corrosion resistance. It makes passive layer of chromium oxide on the alloy's surface. X-ray photoelectron spectroscopy (XPS) analysis shows that this passive layer consists of Cr_2O_3 oxide with some minor contributions from Co and Mo oxides. The same type of films exists on other metallic biomaterials – stainless steel, titanium alloys and serves as a barrier to corrosion process in alloy systems [7 – 9]. To achieve both good corrosion and wear resistance layers on the surface of CoCr alloys are widely used surface modification methods as ion implantation, plasma immersion ion implantation and plasma nitriding, high intensity plasma ion nitriding [5, 9 – 11].

Plasma nitriding is one of the surface treatments type, used to improve materials mechanical characteristics, hardness, fatigue or creep resistance. The nitrogen inserted in alloy during nitriding changes surface chemical composition. During nitriding the expanded austenite phase (γN) can be formed on the surface of CoCr alloys. Similar to nitriding of austenitic stainless steel, insertion of nitrogen into the original lattice on interstitial site, a lattice expansion and an anomalous diffusion is observed for CoCr [12]. The understanding of N diffusion mechanism is very important. This diffusion behavior could be explained on a microscopic level with trapping at Cr atoms or on a macroscopic level assuming a nitrogen concentration dependant diffusivity [12]. The nitrogen contents are presumably obtained due to the high affinity between N and Cr, where N is believed to reside in the immediate vicinity of the supposedly randomly distributed Cr atoms, implying that only short range ordering of Cr and N occurs. There are strong indications that the tightly bound N interacts with Cr, which leads to nitrogen trapping [13 – 15].

The TD model is based on the assumption that chromium atoms act as trap sites for the nitrogen and, once all traps are saturated a faster diffusion is observed [16]. According to the similar studies in literature [12, 16] it was found that the stainless steel nitrided layers are thicker than nitrided CoCrMo alloys layers. This difference is explained by Cr content. So, it is expected that it takes longer time to saturate all Cr traps for CoCrMo (compare to ASS) exhibiting thinner nitrided layers due to more Cr content in CoCrMo [16].

In this work we are applying the Trapping-detrapping model for CoCrMo in order to show that the main

*Corresponding author. Tel.: +370-37-300349; fax: +370-37-456472.
E-mail address: *galdikas@ktu.lt* (A. Galdikas)

mechanisms of nitrogen penetration are the same as in stainless steel. Experimental depth profiles of nitrogen after nitriding CoCrMo alloy show "plateu" (see Fig. 1) which cannot be obtained by ordinary diffusion equations. Quite similar behavior is observed for nitriding of stainless steel. Trapping-detrapping model for stainless steel proposed by S. Parascondola at [17, 18] and other authors [19, 20] for analysis nitrogen penetration in stainless steel. Because, chromium plays the main role in stainless steel we propose that the same mechanism can take place for CoCrMo alloys.

2. THE MODEL

Trapping is based on the fact that the Cr atoms act as trap sites for nitrogen. Trapped nitrogen atoms can be detrapped with activation energy of detrapping E_b and then participate in diffusion process. Total amount of nitrogen is $N = N_{dif} + N_{trap}$ where N_{dif} is the number of nitrogen atoms which participate in diffusion and N_{trap} is the number of nitrogen atoms, which are in traps. The final trapping – detrapping model equations [17] modified for plasma nitriding by adding adsorption term $\alpha \cdot j_0\left(N_0 - N_{dif} - N_{trap}\right)$ [22] are:

$$\frac{\partial N_{dif}(x,t)}{\partial t} = D\frac{\partial^2 N_{dif}(x,t)}{\partial x^2} + \alpha \cdot j_0\left(N_0 - N_{dif} - N_{trap}\right) - S(x,t)$$

$$\frac{\partial N_{trap}(x,t)}{\partial t} = S(x,t) = \tag{1}$$

$$= 4\pi R_t D\left[N_{dif}(x,t)(H_t - N_{trap}(x,t)) - \zeta N_0 N_{trap}(x,t)e^{-\frac{E_B}{k_B T}}\right]$$

where H_t is chromium concentration, N_0 is atom density matrix, R_t is trapping radius equal lattice constant, $D = D_0 \exp(-E_A/kT)$ is diffusion coefficient which follows Arrhenius law, D_0 is preexponential factor of diffusion, E_A is diffusion activation energy, ξ is number of places near trap there nitrogen could be catched caught, T is temperature, k_B is Boltzmann constant, α is the sticking coefficient of nitrogen to the surface and j_0 is the flux of nitrogen atoms to the surface.

For simulations the differential equations eq. (1) are solved numerically. Eq. (1) are expressed in finite increments as:

for surface layer : $k = 0$

$$\frac{\partial N_{dif}^{(0)}}{\partial t} = -\frac{D}{h^2}\left(N_{dif}^{(1)} - N_{dif}^{(0)}\right) - S^{(0)} + \alpha \cdot j_0\left(N_0 - N_{dif}^{(0)} - N_{trap}^{(0)}\right) \tag{2}$$

$$\frac{\partial N_{trap}^{(0)}}{\partial t} = S^{(0)} = 4\pi R_t D\left[N_{dif}^{(0)}(H_t - N_{trap}^{(0)}) - N_0 N_{trap}^{(0)} e^{\frac{-E_B}{k_B T}}\right]. \tag{3}$$

And for *other* layers $k \geq 1$

$$\frac{\partial N_{dif}^{(k)}}{\partial t} = -\frac{D}{h^2}\left(N_{dif}^{(k+1)} - N_{dif}^{(k-1)} - 2N_{dif}^{(k)}\right) - S^{(k)}; \tag{4}$$

$$\frac{\partial N_{trap}^{(k)}}{\partial t} = S^{(k)} = 4\pi R_t D\left[N_{dif}^{(k)}(H_t - N_{trap}^{(k)}) - N_0 N_{trap}^{(k)} e^{\frac{-E_B}{k_B T}}\right], \tag{5}$$

where $N_i^{(k)}$ is number of nitrogen atoms in i-th state in k-th monolayer.

3. RESULS AND DISCUSSION

The experimental results were analyzed by the proposed model. The experimental depth profiles of nitrogen taken from refs. [2, 4] and obtained by GDOES after plasma nitriding of CoCrMo alloy (medical grade alloy D30) at 400 °C for different nitriding times 4 h, 6 h and 20 h are presented in Fig. 1 (points). The alloy was nitrided in a low – pressure (~ 60 mTorr) radio – frequency plasma under a gas mixture of 60 % N_2 – 40 % H_2 [4].

The plateau is seen in all curves which cannot be fitted by simple diffusion models. The similar profiles for nitrided stainless steel are fitted by trapping-detrapping models [17 – 20]. We suggest the same mechanism for CoCrMo alloy.

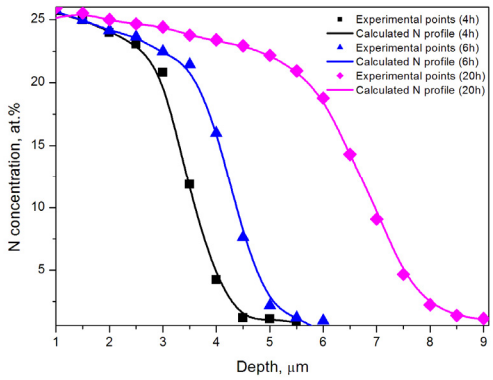

Fig. 1. Experimental (points) [2] and calculated (lines) nitrogen concentration depth profiles obtained at different nitriding times (4 h, 6 h and 20 h)

The nitrogen depth profiles in CoCrMo were calculated by solving Eqs. (2) – (5). In order to fit the experimental curves the calculations were performed by varying two parameters: diffusion coefficient D and activation energy of detrapping E_B. Other parameters were kept as constants and found from the experiment [2] or literature data [17]. Those parameters are listed in Table 1.

Table 1. The values of parameters used in calculations

The parameters from the literature [17]	Parameters found by fitting
$E_A = 1.1$ eV [6] $R_t = 0.38\times10^{-7}$ cm $N_0 = 7.29\times10^{22}$ cm^{-3} $Ht = 2.17242\times10^{22}$ cm^{-3}	$E_B = 0.45$ eV Diffusion coefficients:

Nitriding time, h	D_0, cm^2/s	D, $\times10^{-11}$ cm^2/s
4	0.0116	6.71566
6	0.0105	6.07883
20	0.008	4.63149

The calculation results are presented in Fig. 1 (solid lines) together with the experimental points [2]. All three calculated depth profiles (4 h, 6 h and 20 h of nitriding) are in a good agreement with the experiment. However, in order to get the best fit for all three experimental depth

profiles it was necessary to change diffusion coefficient (other parameters remain as constants for all three cases). The best fitting results were obtained with the following diffusion coefficients, listed in Table 1. It is seen from the obtained values of diffusion coefficients that they decrease with increase of nitriding time. This may be influenced by concentration of nitrogen. With the increase of nitriding time the concentration of nitrogen increases and it means that diffusion coefficient decreases with increase of nitrogen concentration.

According to the Einstein-Smoluchowski relation the diffusion coefficient is inversely proportional to the nitrogen concentration. To check Einstein-Smoluchowski relation for our case, the obtained values of diffusion coefficients were plotted versus parameter $1/C_N$. C_N is total concentration of nitrogen atoms in diffusion and trapped sites integrated over all monolayers.

The plot is presented in Fig. 2. All three points are in one line and confirm assumption that diffusion coefficient depends on concentration according to Einstein-Smoluchowski relation $D \propto 1/C_N$. The line of Fig. 2 is fitted by a function $D_0(C_N) = 0.0058/C_N + 0.0042$. Analyzing the dependence total nitrogen concentration on time (from Fig. 1) it was found the following function $C_N(t) = 0.4416\, t^{0.4231}$. Combining the last two relations the dependence of diffusion coefficient on time can be expressed as $D_0(t) = 0.0013\, t^{-0.4231} + 0.0042$ (for experimental conditions described here). Using this expression the depth profiles of nitrogen for any nitriding time can be calculated.

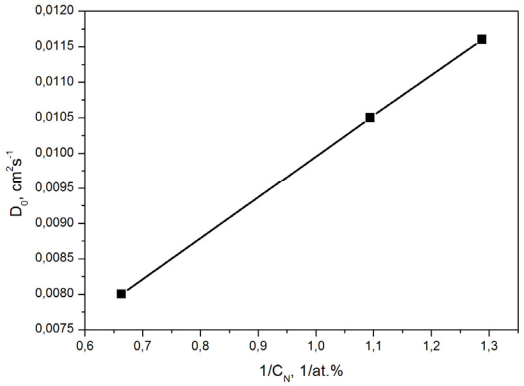

Fig. 2. Function of obtained by fitting D values versus $1/C_N$

The calculated nitrogen depth profiles at different moments of time including the initial stages of nitriding are presented in Fig. 3. It is seen that at initial stages of nitriding the shapes of curves are exponential. But it does not necessary means that at that stages the simple diffusion mechanisms prevail.

In Fig. 4 there are presented depth profiles where the curves for the initial stages of nitriding are detailed into profiles of nitrogen in trapping sites N_{trap} and diffusing nitrogen N_{dif}. It is seen that even profiles of N_{trap} are exponential. Almost all amount of nitrogen is in trapping sites from the beginning of process and only small amount nitrogen belongs to N_{dif}. At later stages, approximately after 30 min. of nitriding, as it is seen in Fig. 3, the shapes of curves start to change and after approximately of 1 h of nitriding the plateau starts to be observed. From the analysis of Fig. 3 and Fig. 4 the formation of plateau can be understood as: the plateau starts to be formed when nitrogen occupies all possible trapping sites whose amount depends on Cr concentration. This is seen in kinetics of nitrogen surface concentration which is plotted in Fig. 5.

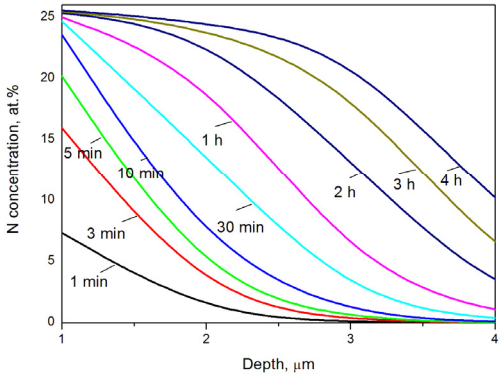

Fig. 3. The calculated nitrogen depth profiles at different moments of time

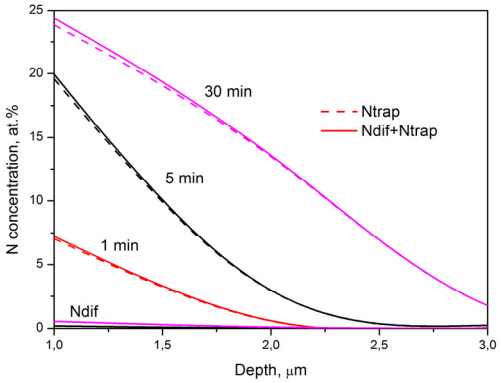

Fig. 4. The calculated nitrogen depth profiles of total nitrogen, nitrogen in trap sites N_{trap} and diffusing nitrogen N_{dif} at different moments of time

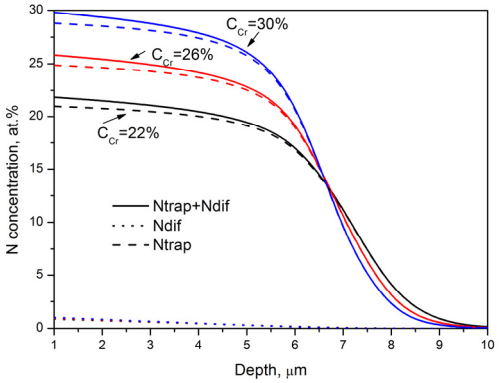

Fig. 5. The dependence of nitrogen surface concentration on nitriding time

Nitrogen surface concentration increases rapidly at the initial stages of nitriding processes and later slowly approaches steady state value which is determined by trapping sites of Cr atoms.

The influence of Cr concentration is shown in Fig. 6. Diffusing nitrogen N_{dif} profile has exponential shape as is

predicted by Fick's diffusion equation term and is almost independent of chromium concentration. Nitrogen in trapping sites N_{trap} strongly depends on Cr concentration and this dependence is reflected in total nitrogen depth profile. The strong dependence on Cr content for total nitrogen N profile is observed in "plateau" region, in deeper layers this dependence is less. With increase of Cr concentration slightly decreases the nitrogen penetration depth as more nitrogen is in trapping sites and cannot diffuse.

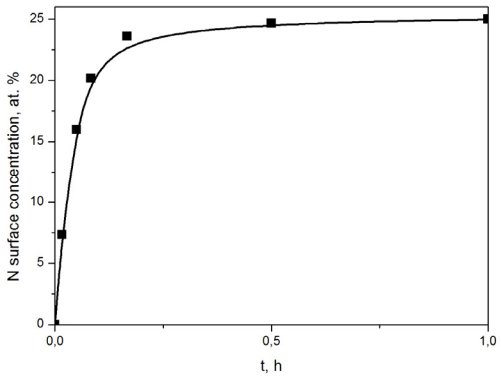

Fig. 6. The nitrogen depth profiles of total nitrogen, nitrogen in trap sites N_{trap} and diffusing nitrogen N_{dif} calculated for different concentrations of chromium. The nitriding time is 20 h

The influence of detrapping activation energy E_b is analyzed in Fig. 7. The nitrogen depth profiles of total N nitrogen, nitrogen in tapping sites N_{trap} and diffusing nitrogen N_{dif} are calculated by varying E_b. Both N_{trap} and N_{dif} depend on E_b. With increase E_b the N_{trap} increases and N_{dif} decreases. The variation of E_b strongly influences the profile of total nitrogen at deeper layers. The penetration depth on nitrogen increases with decrease of E_b because in that case more nitrogen atoms can be detrapped.

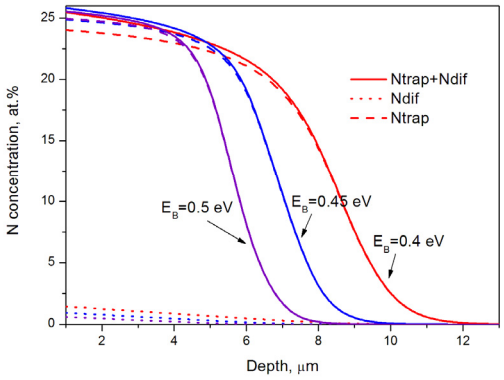

Fig. 7. The nitrogen depth profiles of total nitrogen, nitrogen in trap sites N_{trap} and diffusing nitrogen N_{dif} calculated for different values of detrapping activation energy E_b. The nitriding time is 20 h

4. CONCLUSIONS

1. The nitrogen penetration during plasma nitriding of CoCrMo alloy can be explained by trapping-dettraping mechanism and nitrogen depth profile, taken from literature, can be fitted by equations of proposed model.
2. The nitrogen diffusion coefficient in nitrided CoCrMo alloy depends on nitrogen concentration according to Einstein-Smoluchowski relation $D \propto 1/C_N$.
3. The trapping-detrappining mechanism starts to act from the very beginning of nitriding process and the mechanism of Fick's diffusion is secondary. The plateau in nitrogen depth profile starts to be formed when nitrogen occupies all possible trapping sites whose amount is determined by Cr concentration.
4. The penetration depth of nitrogen increase with decrease of detrapping activation energy and slightly decreases with increase of Cr concentration.

Acknowledgments

This research was partially funded by a grant (No. MIP-030/2013) from the Research Council of Lithuania.

REFERENCES

1. **Çelik, A., Bayrak, Ö., Alsaran, A., Kaymaz, İ., Yetim, A. F.** Effects of Plasma Nitriding on Mechanical and Tribological Properties of CoCrMo Alloy *Surface and Coatings Technology* 202 2008: pp. 2433 – 2438. http://dx.doi.org/10.1016/j.surfcoat.2007.08.030
2. **Pichon, L., Okur, S., Ozturk, O., Riviere, J. P., Drouet, M.** CoCrMo Alloy Treated by Floating Potential Plasma Assisted Nitriding and Plasma Based Ion Implantation: Influence of the Hydrogen Content and of the Ion Energy on the Nitrogen Incorporation *Surface & Coatings Technology* 204 2010: pp. 2913 – 2918.
3. **Santavirta, S., Konttinen, Y. T., Lappalainen, R., Anttila, A., Goodman, S. B., Lind, M., Smith, L., Takagi, M., Gdmez-Barrena, E., Nordsletten, L., Xu, J. W.** Material in Total Joint Replacement *Current Orthopaedics* 12 1998: pp. 51 – 57. http://dx.doi.org/10.1016/S0268-0890(98)90008-1
4. **Öztürk, O., Okur, S., Pichon, L., Liedke, M. O., Riviere, J. P.** Magnetic Layer Formation on Plasma Nitrided CoCrMo Alloy *Surface & Coating Technology* 205 2011: pp. 280 – 285.
5. **Wei, R., Booker, T., Rincon, C., Arps, J.** High-intensity Plasma Ion Nitriding of Orthopedic Materials. Part I. Tribological Study *Surface & Coatings Technology* 186 2004: pp. 305 – 313.
6. **Lutz, J., Lehmann, A., Mändl, S.** Nitrogen Diffusion in Medical CoCrNiW Alloys after Plasma Immersion Ion Implantation *Surface & Coatings Technology* 202 2008: pp. 3747 – 3753.
7. **Skolek-Stefaniszyn, E., Kaminski, J., Sobczak, J., Wierzchon, T.** Modifying the Properties of AISI 316L Steel by Glow Discharge Assisted Low-temperature Nitriding and Oxynitriding *Vacuum* 85 2010: pp. 164 – 169.
8. **Öztürk, O., Türkan, U., Eroğlu, A. E.** Metal Ion Release from Nitrogen Ion Implanted CoCrMo Orthopedic Implant Material *Surface & Coatings Technology* 200 2006: pp. 5687 – 5697.
9. **Lanning, B. R., Wei, R.** High Intensity Plasma Ion Nitriding of Orthopedic Materials. Part II. Microstructural Analysis *Surface & Coatings Technology* 186 2004: pp. 314 – 319. http://dx.doi.org/10.1016/j.surfcoat.2004.02.047

10. **Ortega-Saenza, J. A., Hernandez-Rodrigueza, M. A. L., Ventura-Sobrevillaa, V., Michalczewski, R., Smolik, J., Szczerek, M.** Tribological and Corrosion Testing of Surface Engineered Surgical Grade CoCrMo Alloy *Wear* 271 2011: pp. 2125 – 2131.
11. **Lutz, J., Mändl, S.** Reduced Tribocorrosion of CoCr Alloys in Simulated Body Fluid after Nitrogen Insertion *Surface & Coatings Technology* 204 2010: pp. 3043 – 3046.
12. **Lutz, J., Mändl, S.** Effect of Ion Energy and Chemistry on Layer Growth Processes during Nitriding of CoCr Alloys Nuclear *Instruments in Physics Research B* 267 2009: pp. 1522 – 1525.
13. **Oddershede, J., Christiansen, T. L., Ståhl, K., Somers, M. A. J.** Extended X-ray Absorption Fine Structure Investigation of Nitrogen Stabilized Expanded Austenite *Scripta Materialla* 62 2010: pp. 290 – 293.
14. **Oddershede, J., Christiansen, T. L., Ståhl, K., Somers, M. A. J.** EXAFS Investigation of Low Temperature Nitrited Stainless Steel *Journal of Materials Science* 43 2008: pp. 5358 – 536.
15. **Christiansen, T. L., Somers, M. A. J.** Low-temperature Gaseous Surface Hardening of Stainless Steel: the Current Status *International Journal of Materials Research* 100 2009: pp.1361 – 1377.
16. **Okur, S.** Structural Compositional and Mechanical Characterization of Plasma Nitrited CoCrMo Alloy. *PhD Thesis in Physics/IZTECH* 2009: 96 p.
17. **Martinavičius, A., Abrasonis, G., Möller, W., Templier, C., Rivière, J. P., Declémy, A., Chumlyakov, Y.** Anisotropic Ion-enhanced Diffusion during Ion Nitriding of Single Crystalline Austenitic Stainless Steel *Journal of Applied Physics* 105 2009: pp. 093502 – 093502-7.
18. **Parascandola, S., Möler, W., Williamson, D. L.** The Nitrogen Transport in Austenitic Stainless Steel at Moderate Temperatures *Applied Physics Letters* 76 2000: p. 2194.
19. **Möller, W., Parascandola, S., Telbizova, T., Günzel, R., Richter, E.** Surface Processes and Diffusion Mechanisms of Ion Nitriding of Stainless Steel and Aluminium *Surface and Coatings Technology* 136 2001: pp. 73 – 79.
20. **Abrasonis, G., Möller, W., Ma, X. X.** Anomalous Ion Accelerated Bulk Diffusion of Interstitial Nitrogen *Physical Review Letters* 96 2006: p. 065901.
21. **Abrasonis, G., Riverie, J. P., Templier, C., Declemy, A., Pranevicius, L., Milhet, X.** Ion Beam Nitriding of Single and Polycrystalline Austenitic Stainless Steel *Applied Physics* 97 2005: p. 083531.
22. **Moskalioviene, T., Galdikas, A., Rivière, J. P., Pichon, L.** Modeling of Nitrogen Penetration in Polycrystalline AISI 316L Austenitic Stainless Steel during Plasma Nitriding *Surface & Coatings Technology* 205 2011: pp. 3301 – 3306.